MULTI-AGENT STEREOVISION SENSITIVITY ANALYSIS FOR RENDEZVOUS WITH NON-COOPERATIVE TARGETS

Kaitlin Dennison[1*] and Simone D'Amico[1]; [1]Stanford University, Stanford, CA 94305; [*]kdenn@stanford.edu

Abstract. *Multi-agent stereovision is a low-power, low-computation, and readily-available alternative to LiDAR and stereophotoclinometry, which is critical to enable more autonomous rendezvous missions in the future. The sensitivity of multi-agent stereovision is evaluated with respect to several variables including observer relative position, measurement and image corruption, and observer state uncertainty. This analysis informs distributed space system geometry, navigation requirements, and necessary measurement accuracy to enable missions to rendezvous with an arbitrary target.*

Introduction. State of the art space-rendezvous mission concepts rely heavily on a priori models of their targets or LiDAR for optical navigation and shape estimation.[1–4] Distributed space systems,[5,6] which are becoming increasingly popular for their flexibility and boost in observability, introduce an alternative to a priori models and LiDAR: multi-agent stereovision (MASV).[7,8] This paper evaluates the precision, accuracy, and robustness of MASV for rendezvous with a non-cooperative target. It also serves as a reference for distributed space system formation design to optimize MASV for natural and man-made targets of varying size.

LiDAR, binocular (stereovision) cameras, and sequential stereovision are often used to recover depth to a target without an a priori model. While LiDAR has high precision, it has high power requirements and demands a balance of trade-offs between moving parts, measurement spread, and observability range.[3,9] Binocular cameras and sequential stereovision have lower power requirements compared to LiDAR. However, binocular cameras have a short observability range, sequential stereovision does not handle target motion well, and both have lower precision than LiDAR.[3,7,10]

The proposed solution is to implement MASV using a distributed space system of multiple observing spacecraft, each equipped with a monocular camera. A surface map of the target can be recovered with low power and cost, albeit with lower accuracy, compared to LiDAR.[2,8,11] However, accuracy and range are improved with respect to binocular cameras because MASV has the ability to widen the baseline between observers.[12] Additionally, MASV can mitigate motion of the target between images with proper clock synchronization. A downside of stereovision in general is that camera state estimates are needed for full depth recovery and the state estimate uncertainty constrains measurement accuracy and precision.[8]

MASV is well-studied in the context of agent relative position, image measurement uncertainty, and triangulation techniques.[12–15] However, there are two gaps that must be filled to make MASV readily applicable to the space rendezvous domain. One, a sensitivity analysis of MASV for space applications is missing in literature. Sensitivity to camera state knowledge and relative positions of multiple observers are especially lacking. Two, space-rendezvous with respect to poorly-known asteroid and man-made objects and harmonization of associated techniques are typically siloed in literature. This paper performs the simulations and analysis necessary to fill these gaps and thus enable a greater number of space missions in the future by aiding system level and mission design tasks.

Figure 1. A synthetic image of asteroid 433 Eros.

Methodology. Two different space environments are simulated to perform the analysis. One with asteroid 433 Eros[8] as the target and the other with the Tango spacecraft from the PRISMA mission[16] as the target. Example synthetic images of both are shown in Figures 1 and 2. By having two starkly-different targets, trends that can be generalized to both can potentially be generalized to other targets.

Two point types are detected in both targets: visible shape model vertices and keypoint descriptors. Shape model vertices are projected into the image frame and provide ground truth. SIFT[17] and ORB[18] are used for Eros and Tango, respectively. The keypoints are matched using the 3D ray-traced position of each 2D feature center through the model of the respective target.[7] The 3D ray-traced positions are also used to quantify the stereovision error. Stereovision 3D points are computed using iterative nonlinear triangulation as described by Hartely[13] and in Stacey et al.[8] MASV performance is assessed with respect to seven variables.

The first two variables are, one, the number of observers and, two, their angular separation in a string

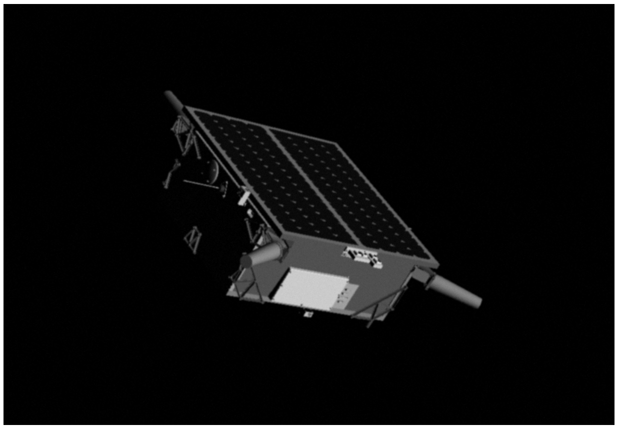

Figure 2. A synthetic image of the Tango spacecraft.

of pearls formation. Of all the variables, these have the greatest impact on mission design because the number and relative position of the spacecraft heavily influence guidance, navigation, and control.[8, 19] Increasing the number of observers (and, thus, the number of 2D measurements) and the angular separation between them should lead to improved 3D reconstruction.[12, 13] However, the size and extent of that improvement is unclear in literature.

Next is the target angular size θ, which relates to the amount of the image that the target encompasses and the surface detail resolution. The relationship between θ, the distance to the target d, the maximum width of the target w, and the camera focal length f is given by

$$\theta = 2 \arctan \frac{w}{2(f-d)}. \tag{1}$$

Eq. (1) is derived from the Gaussian lens equation and the equation for the field of view.[20] As θ increases and approaches or surpasses the camera field of view, more details become visible and more individual surface points become distinct, lessening the influence of measurement noise.

Measurement noise and image corruption are the fourth and fifth variables. No feature detection algorithm or camera is perfect. Measurement noise is modeled as zero-mean Gaussian error added to the 2D pixel measurements. The image corruption methods considered are Gaussian white noise, speckle noise, and Gaussian blurring. Measurement noise is only used for the shape model vertex points while image corruption is only used for the keypoints.

The final two variables are the observer position and attitude uncertainty. The study by Stacey et al.[8] shows how MASV estimates can be used to support simultaneous navigation and characterization of an unknown asteroid. Ultimately, the stereovision accuracy was constrained by the spacecraft state estimate accuracy. Thus, stereovision error tolerances inform navigation error tolerances it is critical to understand their relationship.

Preliminary Results. Fig. 3 shows preliminary results for a simulation of three spacecraft observing Eros and Tango for a subset of variables. The observer-target geometries and camera models are the same between the Eros and Tango setups. The residual is plotted as the percentage of the maximum width of the target.

When the size of the target is accounted for, the relationship between variable and residual is the largely the same. This indicates that the distributed space system and the measurement method can be optimized to achieve the desired results regardless of the target. An analysis of the remaining variables will provide further insight.

References.

[1] D. A. Lorenz, R. Olds, A. May, C. Mario, M. E. Perry, E. E. Palmer, *et al.*, "Lessons learned from OSIRIS-REx autonomous navigation using natural feature tracking," in *IEEE Aerospace Conference*, (Big Sky, MT, USA), Mar. 2017.

[2] S. Watanabe, M. Hirabayashi, N. Hirata, N. Hirata, R. Noguchi, Y. Shimaki, *et al.*, "Hayabusa2 arrives at the carbonaceous asteroid 162173 Ryugu—A spinning top–shaped rubble pile," *Science*, vol. 364, pp. 268–272, Apr. 2019.

[3] R. Opromolla, G. Fasano, G. Rufino, and M. Grassi, "A review of cooperative and uncooperative spacecraft pose determination techniques for close-proximity operations," *Progress in Aerospace Sciences*, vol. 93, pp. 53–72, 2017.

[4] S. Sharma and S. D'Amico, "Neural network-based pose estimation for noncooperative spacecraft rendezvous," *IEEE Transactions on Aerospace and Electronic Systems*, vol. 56, no. 6, pp. 4638–4658, 2020.

[5] H. Sanchez, D. McIntosh, H. Cannon, C. Pires, J. Sullivan, B. O'Connor, and S. D'Amico, "Starling1: Swarm technology demonstration," in *32nd Annual Small Satellite Conference, AIAA/USU*, 2018.

[6] J. Kruger, K. Wallace, A. Koenig, and S. D'Amico, "Autonomous angles-only navigation for spacecraft swarms around planetary bodies," in *IEEE Aerospace Conference*, (Virtual), 2021.

[7] K. Dennison and S. D'Amico, "Comparing optical tracking techniques in distributed asteroid orbiter missions using ray-tracing," in *AAS/AIAA Space Flight Mechanics Meeting*, (Charlotte, NC), Feb. 2021.

[8] N. Stacey, K. Dennison, and S. D'Amico, "Autonomous asteroid characterization through nanosatellite swarming," in *IEEE Aerospace Conference*, (Big Sky, MT, USA), Mar. 2022.

[9] M. Driedger, A. Asgari, and P. Ferguson, "Feasibility of gathering resident space object range measurements using in-orbit observers," *IEEE Journal of Radio Frequency Identification*, 2022.

[10] L. Zhang, F. Zhu, Y. Hao, and W. Pan, "Optimization-based non-cooperative spacecraft pose estimation using stereo cameras during proximity operations," *Applied Optics*, vol. 56, no. 15, pp. 4522–4531, 2017.

[11] GOMSpace, "NanoCam C1U Datasheet," 2016.

[12] M. Hess-Flores, S. Recker, and K. I. Joy, "Uncertainty, baseline, and noise analysis for L1 error-based multi-view triangulation," in *22nd International Conference on Pattern Recognition*, (Stockholm, Sweden), pp. 4074–4079, Aug. 2014.

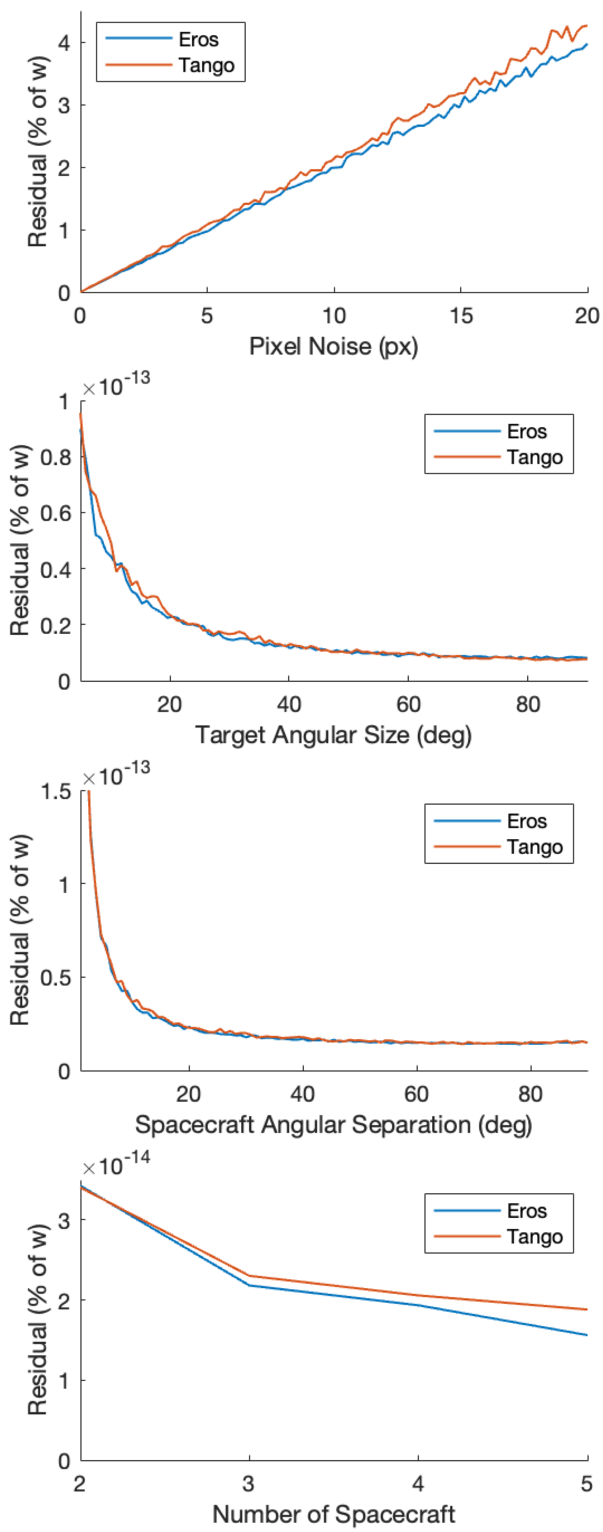

Figure 3. A comparison of stereovision residuals for Eros and Tango as targets. Model vertices were used as points with three spacecraft, 20° angular separation, and 20° target angular size as the defaults.

[13] R. Hartley and A. Zisserman, *Multiple view geometry in computer vision.* Cambridge: Cambridge University Press, 2003.

[14] P. Schmuck and M. Chli, “Multi-UAV collaborative monocular SLAM,” in *IEEE International Conference on Robotics and Automation*, (Marina Bay Sands, Singapore), May 2017.

[15] S. Henry and J. A. Christian, “Absolute triangulation algorithms for space exploration,” 2022.

[16] S. D’Amico, J.-S. Ardaens, and R. Larsson, “Spaceborne autonomous formation-flying experiment on the prisma mission,” *Journal of Guidance, Control, and Dynamics*, vol. 35, no. 3, pp. 834–850, 2012.

[17] D. G. Lowe, “Distinctive image features from scale-invariant keypoints,” *International Journal of Computer Vision*, vol. 60, pp. 91–110, Nov. 2004.

[18] E. Rublee, V. Rabaud, K. Konolige, and G. Bradski, “ORB: An efficient alternative to SIFT or SURF,” in *2011 International Conference on Computer Vision*, (Barcelona, Spain), pp. 2564–2571, Nov. 2011.

[19] C. Lippe and S. D’Amico, “Spacecraft swarm dynamics and control about asteroids,” (University of Strathclyde Glasglow, UK), p. 18, July 2019.

[20] E. Hecht, *Optics, global edition.* Pearson Education UK, 2016.